Nodal Order Parameter in Electron-Doped $Pr_{2-x}Ce_xCuO_{4-\delta}$ Superconducting Films

A. Snezhko and R. Prozorov
Department of Physics & Astronomy and NanoCenter, University of South Carolina, 712 Main Street, Columbia, South Carolina 29208, USA

D. D. Lawrie and R.W. Giannetta
Loomis Laboratory of Physics, University of Illinois at Urbana-Champaign, 1110 West Green Street, Urbana, Illinois 61801, USA

J. Gauthier, J. Renaud, and P. Fournier
Centre de Recherche sur les Propriétés Électroniques de Matériaux Avancés, Département de Physique, Université de Sherbrooke, Sherbrooke, Québec, Canada J1K 2R1

(Received 10 April 2003; published 16 April 2004)

The London penetration depth, $\lambda_{ab}(T)$, is reported for thin films of the electron-doped superconductor $Pr_{2-x}Ce_xCuO_{4-\delta}$ with varying Ce concentration, $x = 0.13$, 0.15, and 0.17. Measurements down to 0.35 K were carried out using a tunnel-diode oscillator with excitation fields applied both perpendicular and parallel to the conducting planes. Films at all three doping levels exhibited power law behavior indicative of d-wave pairing with impurity scattering. These results are fully consistent with previous measurements on single crystals.

DOI: 10.1103/PhysRevLett.92.157005 PACS numbers: 74.25.Nf, 74.72.Jt

It is now generally accepted that the hole-doped high-T_c cuprates exhibit d-wave pairing symmetry [1,2]. For electron-doped materials, several different experiments have recently provided strong evidence for unconventional pairing. These include penetration depth on single crystals [3,4], tricrystal measurements [5], angle resolved photoelectron spectroscopy (ARPES) [6], tunneling [7,8], specific heat [9], and Raman scattering [10]. However, the situation in thin films has been controversial. Tunneling measurements provided evidence for an energy gap [11]. Mutual inductance measurements of the penetration depth $\lambda(T)$ in $Pr_{2-x}Ce_xCuO_{4-\delta}$ (PCCO) films claimed gapped behavior in optimal and overdoped films and a transition to a T^2 power law for underdoped films, indicative of d-wave pairing [12]. More recent measurements on PCCO films grown with a Pr_2CuO_4 buffer layer indicate a nodeless order parameter at all doping levels [13], albeit with a small value of the superconducting gap ($\sim 0.9T_c$ compared to $1.76T_c$ of a weak-coupling BCS value). In this Letter we report measurements of $\lambda(T)$ in PCCO films for several different doping levels and for ac magnetic field excitation both parallel and perpendicular to the conducting planes. We find evidence for a nodal order parameter in all the films studied.

PCCO films of thickness 2500 Å were grown using pulsed laser deposition (PLD) on $LaAlO_3$ and yttria stabilized zirconia substrates. Details of the growth procedure can be found in Ref. [14]. Films were optimized for oxygen content by maximizing T_c for each cerium concentration. X-ray diffractometry showed only a small fraction ($\sim 1\%$) of misaligned PCCO grains with (110) orientation, similar to earlier data obtained on high quality PCCO films [14]. No other peaks from secondary phases were detected in the films studied. Impurity content was assessed from standard four-probe ac resistivity measurements shown in the inset of Fig. 1. Critical temperatures and corresponding cerium doping levels for underdoped, optimally doped, and overdoped films

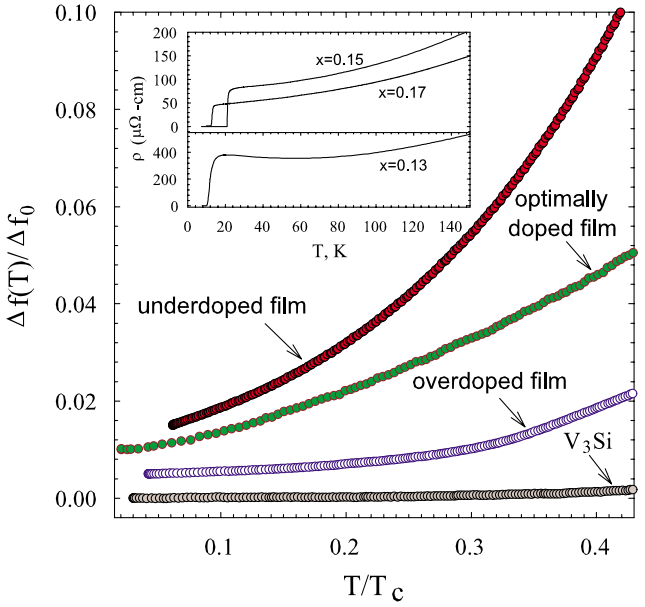

FIG. 1 (color online). Variation of normalized frequency shift [proportional to change in $\lambda_{ab}(T)$] as a function of T/T_c for three $Pr_{2-x}Ce_xCuO_{4-\delta}$ films with ($x = 0.13$, 0.15, and 0.17). Data offsets are used for clarity. Data for V_3Si (an isotropic s-wave superconductor) were taken in the same apparatus. Δf_0 is the total frequency shift when the sample at 0.4 K is inserted into the resonator coil. Inset: Resistivity versus temperature for the same PCCO films.

used in the measurements were $T_c = 9.1$ K ($x = 0.13$), $T_c = 20.5$ K ($x = 0.15$), and $T_c = 11.8$ K ($x = 0.17$), respectively. This doping dependence of T_c is consistent with the known phase diagram for electron-doped superconductors.

Penetration depth measurements were carried out using a 13 MHz tunnel-diode LC resonator [15,16]. The samples were placed on a movable sapphire stage with temperature control from 0.35 to 40 K. When the ac magnetic field is applied perpendicular to the conducting Cu-O planes ($H_{ac} \perp ab$) only in-plane screening currents are induced. In that case, it can be shown that the frequency shift of the resonator is proportional to the change of the in-plane penetration depth, $\Delta f = f(T) - f(0) = G[\lambda_{ab}(T) - \lambda_{ab}(0)]$, where G is a geometrical factor that depends upon the sample shape and volume as well as the coil geometry [15,16]. When $H_{ac} \parallel ab$ there are no demagnetization effects and the oscillator frequency shift is accurately proportional to the susceptibility for a superconducting slab [16],

$$-4\pi\chi = 1 - \frac{2\lambda_{ab}}{d}\tanh\left(\frac{d}{2\lambda_{ab}}\right). \quad (1)$$

In principle, the interplane penetration depth λ_c also contributes to the susceptibility for this field orientation. However, its relative contribution is proportional to $\lambda_c d/\lambda_{ab} w$, where d is the thickness and w is the width [16]. For our films $d/w \sim 10^{-4}$ and $\lambda_c/\lambda_{ab} \sim 25$–$100$ so the λ_c contribution is negligible.

Figure 1 shows data as a function of (T/T_c) for three PCCO films with differing Ce doping levels. In each case the magnetic field was applied perpendicular to the ab plane. Data are offset for clarity. Owing to the very large demagnetization factor in this orientation, it was difficult to reliably determine the calibration constant G relating $\Delta f(T)$ to $\Delta\lambda(T)$. However, the change in frequency, Δf_0, obtained by inserting the sample at its lowest temperature into the resonator, is proportional to the calibration constant G for each individual sample. We have therefore plotted $\Delta f(T)/\Delta f_0$ for each sample to obtain a quantity that is proportional to $\Delta\lambda(T)$ but is independent of sample shape and volume. For comparison we also show data taken in the same apparatus for V_3Si, a weak-coupling isotropic s-wave superconductor. The behavior of $\lambda(T)$ for the PCCO films is markedly different from that obtained for the s-wave material.

The data for an underdoped PCCO film is shown in Fig. 2, along with several fits. The fitting range was chosen up to $0.32T_c$ to ensure the validity of low temperature BCS expression for an s-wave material,

$$\Delta\lambda = \lambda(0)\sqrt{\frac{\pi\Delta_0}{2T}}\exp\left(-\frac{\Delta_0}{T}\right). \quad (2)$$

Here Δ_0 is the value of the energy gap at zero temperature [17]. In each case the small negative offset $A = \lambda(0) -$

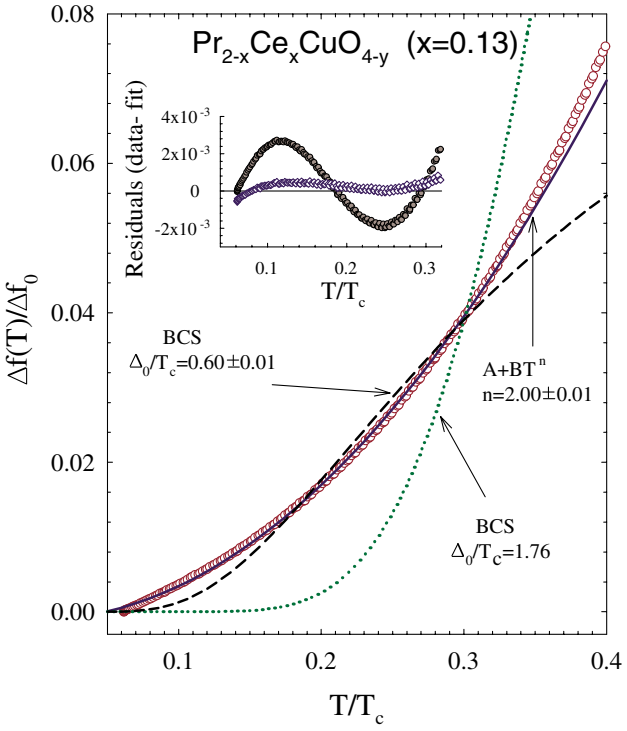

FIG. 2 (color online). Low temperature penetration depth variation in an underdoped PCCO film. The inset shows residuals (experimental data–fit) for the best BCS (solid symbols) and best power law (open symbols) fits. The low temperature exponential s-wave fit is unacceptably poor. The best fit is achieved for the T^n power law with $n = 2.00 \pm 0.01$.

$\lambda(0.4\text{ K})$ was determined as a fitting parameter. The dotted line shows a fit to the standard BCS form with the weak-coupling gap value $\Delta_0/T_c = 1.76$. The dashed curve shows the best fit obtained by allowing Δ_0 to be a free parameter. In this case the extracted value $\Delta_0/T_c = 0.60 \pm 0.01$ is considerably smaller than the weak-coupling BCS value. The solid line is a fit to a power law, $\Delta f \sim A + BT^n$. The best result was achieved with $n = 2.00 \pm 0.01$. The quadratic exponent was observed in single crystals of PCCO and was interpreted as evidence for a gap function with line nodes and unitary limit impurity scattering [3,4,18].

In general it is preferable to analyze the superfluid density, $\rho_s(T) = [\lambda(0)/\lambda(T)]^2$ rather than $\lambda(T)$ directly. ρ_s typically obeys a simple functional form over a wider temperature range than does $\lambda(T)$ itself. For example, in high quality $YBa_2Cu_3O_{7-\delta}$ (YBCO), ρ_s is linear in temperature up to nearly $0.3T_c$ while $\lambda(T)$ departs from linearity above $\sim 0.1T_c$ [15,19]. To obtain ρ_s one must calibrate both $\Delta\lambda(T)$ and $\lambda(0)$, neither of which is easily determined in the $H_{ac} \perp ab$ orientation. These difficulties were overcome by using the $H_{ac} \parallel ab$ data as a reference. Since both configurations probe $\lambda_{ab}(T)$, the $H_{ac} \perp ab$ data was simply scaled to fit the $H_{ac} \parallel ab$ data. The result is shown in Fig. 3 for both optimal and overdoped films as a function of $(T/T_c)^2$. The solid lines

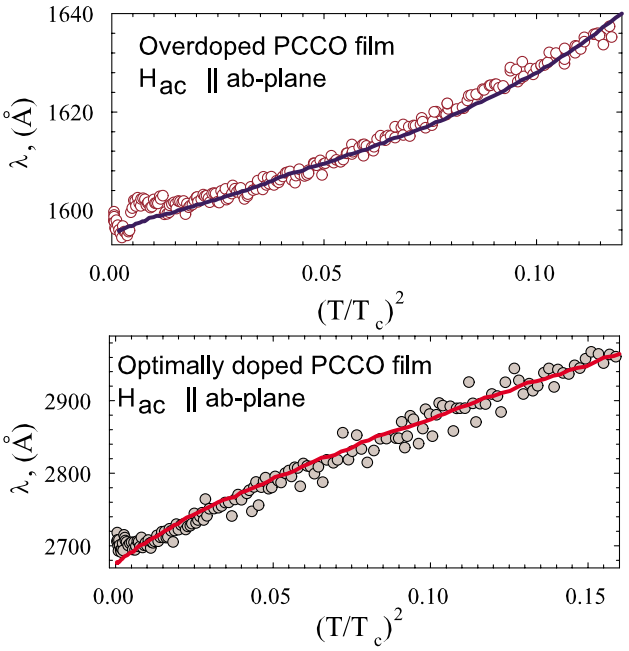

FIG. 3 (color online). $\lambda(T)$ for overdoped (top) and optimally doped (bottom) PCCO films measured in a $H_{ac} \parallel ab$ configuration. Solid lines are data from $H_{ac} \perp ab$ measurements, scaled to agree with $H_{ac} \parallel ab$ data.

represent the suitably scaled $H_{ac} \perp ab$ data. This procedure allowed us to use the much more precise $H_{ac} \perp ab$ data to obtain ρ_s. Since λ is comparable to the film thickness and there is no demagnetizing effect, the total frequency shift in the parallel orientation is very small and the data is correspondingly noisier. $\lambda(T)$ in underdoped films is considerably larger than for optimal or overdoping. As such, the frequency shift was extremely small for the $H_{ac} \parallel ab$ data and the scaling procedure was not possible.

Figure 4 shows ρ_s for the optimally doped PCCO film. The dash-dotted line represents the low temperature BCS expression for $\rho(T)$, with $\Delta_0/T_c = 1.76$ for weak coupling. A fitting range up to $0.32T_c$ was chosen to ensure the validity of the BCS expression. The solid line is a fit to the "dirty d-wave" form $\rho_s \sim 1 - AT^2/(T^* + T)$ with $T^* = 0.21T_c$ [18]. In this model T^* is a measure of the rate of unitary limit impurity scattering in a d-wave superconductor. The power law provides a clearly superior fit to the data. Moreover, the figure shows that ρ_s exhibits a nearly linear variation with temperature above T^*, indicative of a pure d-wave state. Our earlier measurements with single crystals showed strictly T^2 behavior, suggesting that this optimally doped film is among the cleanest of PCCO samples. The inset shows the dependence of the calculated $\rho_s(T)$ upon the choice of $\lambda(0)$. The value $\lambda(0) = 2600$ Å was obtained directly from the parallel field measurement and used for the main plot. For comparison, Kim *et al.* [13] obtained $\lambda(0) \sim$ 1500–1700 Å for their optimally and overdoped PCCO

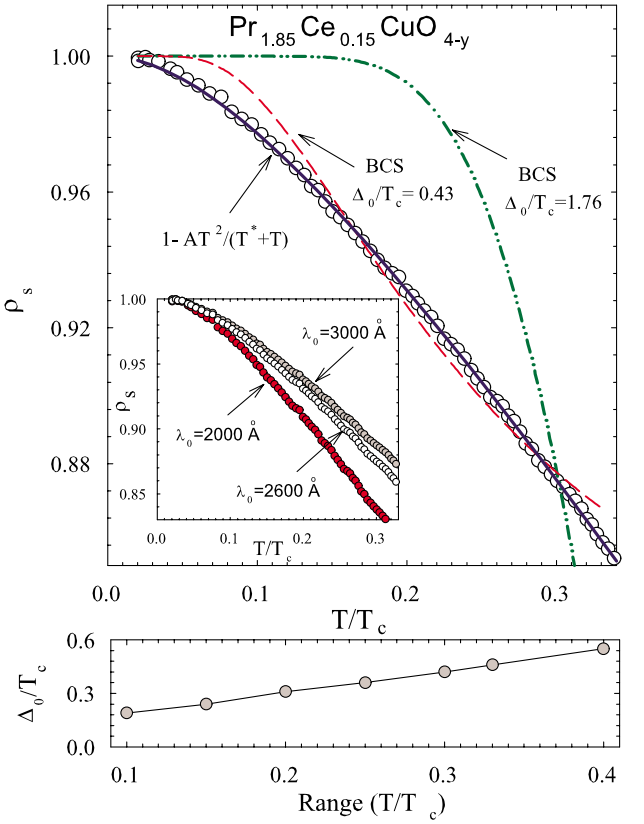

FIG. 4 (color online). $\rho_s(T)$ vs T/T_c for an optimally doped PCCO film. Solid line is a fit to the dirty d-wave form. Dash-dotted line is a fit to the weak-coupling BCS expression. Dashed curve is a fit using the BCS form with energy gap as a free parameter. Inset: $\rho_s(T)$ for three choices of $\lambda(0)$. Lower panel: Energy gap obtained by fitting over successively smaller temperature intervals.

films. A smaller value of $\lambda(0)$ reduces the effective power law exponent and makes the calculated $\rho_s(T)$ even more linear. Although the weak-coupling gap value gives an unsatisfactory fit, it is possible that a much smaller energy gap exists. A reduced energy gap implies that the range over which $\lambda(T) \sim \exp(-\Delta/T)$ is also smaller. We found that by fitting over successively smaller temperature intervals, the fitted gap dropped continuously as shown by the lower panel. The dashed line in Fig. 4 shows the best exponential fit with energy gap as a free parameter. The gap so obtained is $\Delta_0/T_c = 0.43$, but the power law fit is superior.

Figure 5 shows ρ_s for an overdoped PCCO film. In this case we have plotted the data against $(T/T_c)^2$. The solid line is a pure T^2 power law and the dash-dotted line is the BCS form with the weak-coupling energy gap. The lower panel shows the energy gap obtained by fitting the data to the BCS form, but as a function of the fitting range. If an exponential is the best fit then the gap so obtained should saturate as the fitting range is reduced. The fitted energy gap does show a tendency to saturate at $\Delta_0/T_c \sim 0.2$. The dashed line in the main figure shows the exponential BCS

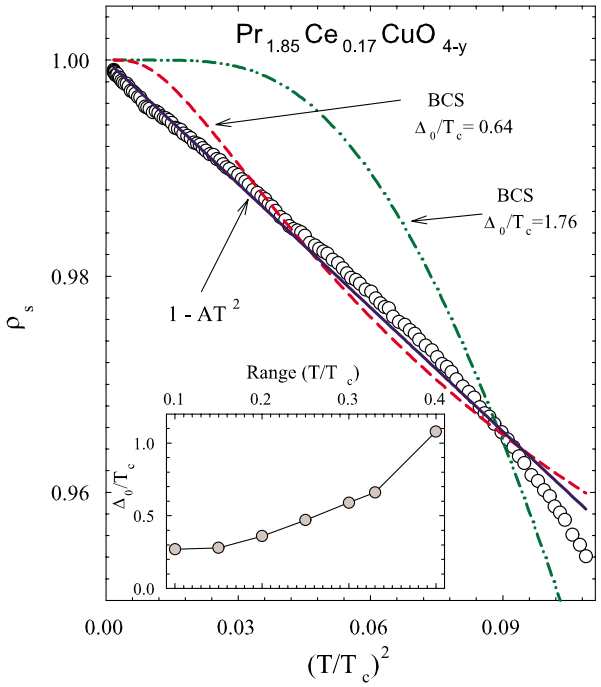

FIG. 5 (color online). $\rho_s(T)$ vs $(T/T_c)^2$ in an overdoped PCCO film. Solid line is a pure T^2 power law. Dash-dotted curve is a weak-coupling BCS expression. Dashed curve is a fit using the BCS form with Δ_0/T_c as a free parameter. Inset: Reduced energy gap obtained by fitting over successively smaller temperature intervals.

fit using Δ_0 as a free parameter. The quadratic power law still provides a superior fit.

Our results differ from those reported in Ref. [13] on buffered PCCO films, where a finite energy gap in a range of $0.3 \leq \Delta_0/T_c \leq 1$ was obtained for various doping levels. In a related earlier study by the same group [12] a transition from *s*- to *d*-wave pairing was reported. For comparable cerium content, the molecular beam epitaxy grown PCCO films investigated in that work had lower residual resistivities and higher superconducting transition temperatures than single crystals, polycrystalline materials, and PLD-grown films [20]. This disparity suggests that details of chemical composition and possibly film morphology are crucial variables. To address the chemical homogeneity issue we calculated the effective penetration depth for a sample containing a distribution of transition temperatures, using the weak-coupling *s*-wave BCS approach. The calculation showed that in order to mimic a quadratic power law the sample would require a linear probability distribution of T_c*s* extending from $T_c(\max)$ down to $T = 0$. Such a distribution is chemically unfeasible and there is no indication of chemical inhomogeneity from the observed superconducting transition widths and transport measurements. Furthermore, $\rho_s(T)$ for the optimally doped film agreed quite closely with our earlier measurements on single crystals. Another source of discrepancy is paramagnetic background coming from the substrate that could mask power law behavior at low temperatures. In the present work, the substrate contribution was eliminated by measuring it directly after the films were etched. The paramagnetic background tends to decrease the apparent diamagnetic signal and may lead to an apparent *s*-wave behavior as pointed out by Cooper [21].

To summarize, we have determined the superfluid density in optimally doped and overdoped PCCO films using two different magnetic field orientations. In each case a power law yielded a superior fit to an exponential, suggesting the presence of nodes in the energy gap. $\rho_s(T)$ for the optimally doped film showed the first evidence of a linear T component, indicative of a pure *d*-wave state. Although it was not possible to determine $\rho_s(T)$ for the underdoped film, its penetration depth varied quadratically with temperature, again giving evidence of a nodal order parameter in PCCO.

Work at the University of South Carolina was supported by the NSF/EPSCoR under Grant No. EPS-0296165. Work at the University of Illinois was supported by NSF under Grant No. DMR-0101872. P. F. acknowledges the support of CIAR, CFI, the Natural Sciences and Engineering Research Council of Canada, and the Foundation of the Université de Sherbrooke.

[1] D. Van Harlingen, Rev. Mod. Phys. **67**, 515 (1995).
[2] C. C. Tsuei and J. R. Kirtley, Rev. Mod. Phys. **72**, 969 (2000).
[3] R. Prozorov *et al.*, Phys. Rev. Lett. **85**, 3700 (2000).
[4] J. D. Kokales *et al.*, Phys. Rev. Lett. **85**, 3696 (2000).
[5] C. C. Tsuei and J. R. Kirtley, Phys. Rev. Lett. **85**, 182 (2000).
[6] N. P. Armitage *et al.*, Phys. Rev. Lett. **85**, 3696 (2000).
[7] F. Hayashi *et al.*, J. Phys. Soc. Jpn. **67**, 3234 (1998).
[8] A. Biswas *et al.*, Phys. Rev. Lett. **88**, 207004 (2002).
[9] H. Balci *et al.*, Phys. Rev. B **66**, 174510 (2002).
[10] G. Blumberg *et al.*, Phys. Rev. Lett. **88**, 107002 (2002).
[11] L. Alff *et al.*, Phys. Rev. Lett. **83**, 2644 (1999).
[12] J. A Skinta *et al.*, Phys. Rev. Lett. **88**, 207005 (2002).
[13] M. S. Kim, J. A. Skinta, and T. R. Lemberger, Phys. Rev. Lett. **91**, 087001 (2003).
[14] E. Maiser *et al.*, Physica (Amsterdam) **297C**, 15 (1998).
[15] A. T. Carrington *et al.*, Phys. Rev. B **59**, R14 173 (1999).
[16] R. Prozorov *et al.*, Phys. Rev. B **62**, 115 (2000).
[17] J. F. Annett, N. Goldenfeld, and A. J. Leggett, J. Low Temp. Phys. **105**, 473 (1996).
[18] P. J. Hirschfeld and N. Goldenfeld, Phys. Rev. B **48**, 4219 (1993).
[19] W. N. Hardy, D. A. Bonn, and D. C. Morgan, Phys. Rev. Lett. **70**, 3999 (1993).
[20] J. L. Peng *et al.*, Phys. Rev. B **55**, R6145 (1997).
[21] J. R. Cooper, Phys. Rev. B **54**, R3753 (1996).